Cold-Nuclear-Matter Effects on Heavy-Quark Production in $d+$Au Collisions at $\sqrt{s_{NN}} = 200$ GeV

A. Adare,[11] C. Aidala,[37] N. N. Ajitanand,[53] Y. Akiba,[48,49] H. Al-Bataineh,[43] J. Alexander,[53] A. Angerami,[12] K. Aoki,[30,48] N. Apadula,[54] Y. Aramaki,[10,48] E. T. Atomssa,[31] R. Averbeck,[54] T. C. Awes,[44] B. Azmoun,[5] V. Babintsev,[21] M. Bai,[4] G. Baksay,[17] L. Baksay,[17] K. N. Barish,[6] B. Bassalleck,[42] A. T. Basye,[1] S. Bathe,[6,49] V. Baublis,[47] C. Baumann,[38] A. Bazilevsky,[5] S. Belikov,[5,*] R. Belmont,[58] R. Bennett,[54] A. Berdnikov,[51] Y. Berdnikov,[51] J. H. Bhom,[62] D. S. Blau,[29] J. S. Bok,[62] K. Boyle,[54] M. L. Brooks,[33] H. Buesching,[5] V. Bumazhnov,[21] G. Bunce,[5,49] S. Butsyk,[33] S. Campbell,[54] A. Caringi,[39] C.-H. Chen,[54] C. Y. Chi,[12] M. Chiu,[5] I. J. Choi,[62] J. B. Choi,[8] R. K. Choudhury,[3] P. Christiansen,[35] T. Chujo,[57] P. Chung,[53] O. Chvala,[6] V. Cianciolo,[44] Z. Citron,[54] B. A. Cole,[12] Z. Conesa del Valle,[31] M. Connors,[54] M. Csanád,[15] T. Csörgő,[61] T. Dahms,[54] S. Dairaku,[30,48] I. Danchev,[58] K. Das,[18] A. Datta,[37] G. David,[5] M. K. Dayananda,[19] A. Denisov,[21] A. Deshpande,[49,54] E. J. Desmond,[5] K. V. Dharmawardane,[43] O. Dietzsch,[52] A. Dion,[25] M. Donadelli,[52] O. Drapier,[31] A. Drees,[54] K. A. Drees,[4] J. M. Durham,[54] A. Durum,[21] D. Dutta,[3] L. D'Orazio,[36] S. Edwards,[18] Y. V. Efremenko,[44] F. Ellinghaus,[11] T. Engelmore,[12] A. Enokizono,[44] H. En'yo,[48,49] S. Esumi,[57] B. Fadem,[39] D. E. Fields,[42] M. Finger,[7] M. Finger, Jr.,[7] F. Fleuret,[31] S. L. Fokin,[29] Z. Fraenkel,[60,*] J. E. Frantz,[54] A. Franz,[5] A. D. Frawley,[18] K. Fujiwara,[48] Y. Fukao,[48] T. Fusayasu,[41] I. Garishvili,[55] A. Glenn,[32] H. Gong,[54] M. Gonin,[31] Y. Goto,[48,49] R. Granier de Cassagnac,[31] N. Grau,[12] S. V. Greene,[58] G. Grim,[33] M. Grosse Perdekamp,[22] T. Gunji,[10] H.-Å. Gustafsson,[35,*] J. S. Haggerty,[5] K. I. Hahn,[16] H. Hamagaki,[10] J. Hamblen,[55] R. Han,[46] J. Hanks,[12] E. Haslum,[35] R. Hayano,[10] X. He,[19] M. Heffner,[32] T. K. Hemmick,[54] T. Hester,[6] J. C. Hill,[25] M. Hohlmann,[17] W. Holzmann,[12] K. Homma,[20] B. Hong,[28] T. Horaguchi,[20] D. Hornback,[55] S. Huang,[58] T. Ichihara,[48,49] R. Ichimiya,[48] Y. Ikeda,[57] K. Imai,[30,48] M. Inaba,[57] D. Isenhower,[1] M. Ishihara,[48] M. Issah,[58] D. Ivanischev,[47] Y. Iwanaga,[20] B. V. Jacak,[54,†] J. Jia,[5,53] X. Jiang,[33] J. Jin,[12] B. M. Johnson,[5] T. Jones,[1] K. S. Joo,[40] D. Jouan,[45] D. S. Jumper,[1] F. Kajihara,[10] J. Kamin,[54] J. H. Kang,[62] J. Kapustinsky,[33] K. Karatsu,[30,48] M. Kasai,[48,50] D. Kawall,[37,49] M. Kawashima,[48,50] A. V. Kazantsev,[29] T. Kempel,[25] A. Khanzadeev,[47] K. M. Kijima,[20] J. Kikuchi,[59] A. Kim,[16] B. I. Kim,[28] D. J. Kim,[26] E.-J. Kim,[8] Y.-J. Kim,[22] E. Kinney,[11] Á. Kiss,[15] E. Kistenev,[5] D. Kleinjan,[6] L. Kochenda,[47] B. Komkov,[47] M. Konno,[57] J. Koster,[22] A. Král,[13] A. Kravitz,[12] G. J. Kunde,[33] K. Kurita,[48,50] M. Kurosawa,[48] Y. Kwon,[62] G. S. Kyle,[43] R. Lacey,[53] Y. S. Lai,[12] J. G. Lajoie,[25] A. Lebedev,[25] D. M. Lee,[33] J. Lee,[16] K. B. Lee,[28] K. S. Lee,[28] M. J. Leitch,[33] M. A. L. Leite,[52] X. Li,[9] P. Lichtenwalner,[39] P. Liebing,[49] L. A. Linden Levy,[11] T. Liška,[13] H. Liu,[33] M. X. Liu,[33] B. Love,[58] D. Lynch,[5] C. F. Maguire,[58] Y. I. Makdisi,[4] M. D. Malik,[42] V. I. Manko,[29] E. Mannel,[12] Y. Mao,[46,48] H. Masui,[57] F. Matathias,[12] M. McCumber,[54] P. L. McGaughey,[33] N. Means,[54] B. Meredith,[22] Y. Miake,[57] T. Mibe,[27] A. C. Mignerey,[36] K. Miki,[48,57] A. Milov,[5] J. T. Mitchell,[5] A. K. Mohanty,[3] H. J. Moon,[40] Y. Morino,[10] A. Morreale,[6] D. P. Morrison,[5] T. V. Moukhanova,[29] T. Murakami,[30] J. Murata,[48,50] S. Nagamiya,[27] J. L. Nagle,[11] M. Naglis,[60] M. I. Nagy,[61] I. Nakagawa,[48,49] Y. Nakamiya,[20] K. R. Nakamura,[30,48] T. Nakamura,[48] K. Nakano,[48] S. Nam,[16] J. Newby,[32] M. Nguyen,[54] M. Nihashi,[20] R. Nouicer,[5] A. S. Nyanin,[29] C. Oakley,[19] E. O'Brien,[5] S. X. Oda,[10] C. A. Ogilvie,[25] M. Oka,[57] K. Okada,[49] Y. Onuki,[48] A. Oskarsson,[35] M. Ouchida,[20,48] K. Ozawa,[10] R. Pak,[5] V. Pantuev,[23,54] V. Papavassiliou,[43] I. H. Park,[16] S. K. Park,[28] W. J. Park,[28] S. F. Pate,[43] H. Pei,[25] J.-C. Peng,[22] H. Pereira,[14] D. Yu. Peressounko,[29] R. Petti,[54] C. Pinkenburg,[5] R. P. Pisani,[5] M. Proissl,[54] M. L. Purschke,[5] H. Qu,[19] J. Rak,[26] I. Ravinovich,[60] K. F. Read,[44,55] S. Rembeczki,[17] K. Reygers,[38] V. Riabov,[47] Y. Riabov,[47] E. Richardson,[36] D. Roach,[58] G. Roche,[34] S. D. Rolnick,[6] M. Rosati,[25] C. A. Rosen,[11] S. S. E. Rosendahl,[35] P. Ružička,[24] B. Sahlmueller,[38,54] N. Saito,[27] T. Sakaguchi,[5] K. Sakashita,[48,56] V. Samsonov,[47] S. Sano,[10,59] T. Sato,[57] S. Sawada,[27] K. Sedgwick,[6] J. Seele,[11] R. Seidl,[22,49] R. Seto,[6] D. Sharma,[60] I. Shein,[21] T.-A. Shibata,[48,56] K. Shigaki,[20] M. Shimomura,[57] K. Shoji,[30,48] P. Shukla,[3] A. Sickles,[5] C. L. Silva,[25] D. Silvermyr,[44] C. Silvestre,[14] K. S. Sim,[28] B. K. Singh,[2] C. P. Singh,[2] V. Singh,[2] M. Slunečka,[7] R. A. Soltz,[32] W. E. Sondheim,[33] S. P. Sorensen,[55] I. V. Sourikova,[5] P. W. Stankus,[44] E. Stenlund,[35] S. P. Stoll,[5] T. Sugitate,[20] A. Sukhanov,[5] J. Sziklai,[61] E. M. Takagui,[52] A. Taketani,[48,49] R. Tanabe,[57] Y. Tanaka,[41] S. Taneja,[54] K. Tanida,[30,48,49] M. J. Tannenbaum,[5] S. Tarafdar,[2] A. Taranenko,[53] H. Themann,[54] D. Thomas,[1] T. L. Thomas,[42] M. Togawa,[49] A. Toia,[54] L. Tomášek,[24] H. Torii,[20] R. S. Towell,[1] I. Tserruya,[60] Y. Tsuchimoto,[20] C. Vale,[5] H. Valle,[58] H. W. van Hecke,[33] E. Vazquez-Zambrano,[12] A. Veicht,[22] J. Velkovska,[58] R. Vértesi,[61] M. Virius,[13] V. Vrba,[24] E. Vznuzdaev,[47] X. R. Wang,[43] D. Watanabe,[20] K. Watanabe,[57] Y. Watanabe,[48,49] F. Wei,[25] R. Wei,[53] J. Wessels,[38] S. N. White,[5] D. Winter,[12] C. L. Woody,[5] R. M. Wright,[1] M. Wysocki,[11] Y. L. Yamaguchi,[10] K. Yamaura,[20] R. Yang,[22] A. Yanovich,[21] J. Ying,[19] S. Yokkaichi,[48,49] Z. You,[46] G. R. Young,[44] I. Younus,[42] I. E. Yushmanov,[29] W. A. Zajc,[12] and S. Zhou[9]

(PHENIX Collaboration)

[1]Abilene Christian University, Abilene, Texas 79699, USA

[2]Department of Physics, Banaras Hindu University, Varanasi 221005, India

[3]Bhabha Atomic Research Centre, Bombay 400 085, India

[4]Collider-Accelerator Department, Brookhaven National Laboratory, Upton, New York 11973-5000, USA

[5]Physics Department, Brookhaven National Laboratory, Upton, New York 11973-5000, USA

[6]University of California—Riverside, Riverside, California 92521, USA

[7]Charles University, Ovocný trh 5, Praha 1, 116 36, Prague, Czech Republic

[8]Chonbuk National University, Jeonju, 561-756, Korea

[9]Science and Technology on Nuclear Data Laboratory, China Institute of Atomic Energy, Beijing 102413, People's Republic of China

[10]Center for Nuclear Study, Graduate School of Science, University of Tokyo, 7-3-1 Hongo, Bunkyo, Tokyo 113-0033, Japan

[11]University of Colorado, Boulder, Colorado 80309, USA

[12]Columbia University, New York, New York 10027 and Nevis Laboratories, Irvington, New York 10533, USA

[13]Czech Technical University, Zikova 4, 166 36 Prague 6, Czech Republic

[14]Dapnia, CEA Saclay, F-91191, Gif-sur-Yvette, France

[15]ELTE, Eötvös Loránd University, H—1117 Budapest, Pázmány P.s.1/A, Hungary

[16]Ewha Womans University, Seoul 120-750, Korea

[17]Florida Institute of Technology, Melbourne, Florida 32901, USA

[18]Florida State University, Tallahassee, Florida 32306, USA

[19]Georgia State University, Atlanta, Georgia 30303, USA

[20]Hiroshima University, Kagamiyama, Higashi-Hiroshima 739-8526, Japan

[21]IHEP Protvino, State Research Center of Russian Federation, Institute for High Energy Physics, Protvino, 142281, Russia

[22]University of Illinois at Urbana-Champaign, Urbana, Illinois 61801, USA

[23]Institute for Nuclear Research of the Russian Academy of Sciences, prospekt 60-letiya Oktyabrya 7a, Moscow 117312, Russia

[24]Institute of Physics, Academy of Sciences of the Czech Republic, Na Slovance 2, 182 21 Prague 8, Czech Republic

[25]Iowa State University, Ames, Iowa 50011, USA

[26]Helsinki Institute of Physics and University of Jyväskylä, P.O. Box 35, FI-40014 Jyväskylä, Finland

[27]KEK, High Energy Accelerator Research Organization, Tsukuba, Ibaraki 305-0801, Japan

[28]Korea University, Seoul, 136-701, Korea

[29]Russian Research Center "Kurchatov Institute", Moscow, 123098 Russia

[30]Kyoto University, Kyoto 606-8502, Japan

[31]Laboratoire Leprince-Ringuet, Ecole Polytechnique, CNRS-IN2P3, Route de Saclay, F-91128, Palaiseau, France

[32]Lawrence Livermore National Laboratory, Livermore, California 94550, USA

[33]Los Alamos National Laboratory, Los Alamos, New Mexico 87545, USA

[34]LPC, Université Blaise Pascal, CNRS-IN2P3, Clermont-Fd, 63177 Aubiere Cedex, France

[35]Department of Physics, Lund University, Box 118, SE-221 00 Lund, Sweden

[36]University of Maryland, College Park, Maryland 20742, USA

[37]Department of Physics, University of Massachusetts, Amherst, Massachusetts 01003-9337, USA

[38]Institut fur Kernphysik, University of Muenster, D-48149 Muenster, Germany

[39]Muhlenberg College, Allentown, Pennsylvania 18104-5586, USA

[40]Myongji University, Yongin, Kyonggido 449-728, Korea

[41]Nagasaki Institute of Applied Science, Nagasaki-shi, Nagasaki 851-0193, Japan

[42]University of New Mexico, Albuquerque, New Mexico 87131, USA

[43]New Mexico State University, Las Cruces, New Mexico 88003, USA

[44]Oak Ridge National Laboratory, Oak Ridge, Tennessee 37831, USA

[45]IPN-Orsay, Universite Paris Sud, CNRS-IN2P3, BP1, F-91406, Orsay, France

[46]Peking University, Beijing 100871, People's Republic of China

[47]PNPI, Petersburg Nuclear Physics Institute, Gatchina, Leningrad region, 188300, Russia

[48]RIKEN Nishina Center for Accelerator-Based Science, Wako, Saitama 351-0198, Japan

[49]RIKEN BNL Research Center, Brookhaven National Laboratory, Upton, New York 11973-5000, USA

[50]Physics Department, Rikkyo University, 3-34-1 Nishi-Ikebukuro, Toshima, Tokyo 171-8501, Japan

[51]Saint Petersburg State Polytechnic University, St. Petersburg, 195251 Russia

[52]Universidade de São Paulo, Instituto de Física, Caixa Postal 66318, São Paulo CEP05315-970, Brazil

[53]Chemistry Department, Stony Brook University, SUNY, Stony Brook, New York 11794-3400, USA

[54]Department of Physics and Astronomy, Stony Brook University, SUNY, Stony Brook, New York 11794-3400, USA

[55]University of Tennessee, Knoxville, Tennessee 37996, USA

[56]Department of Physics, Tokyo Institute of Technology, Oh-okayama, Meguro, Tokyo 152-8551, Japan

[57]Institute of Physics, University of Tsukuba, Tsukuba, Ibaraki 305, Japan

[58]*Vanderbilt University, Nashville, Tennessee 37235, USA*
[59]*Waseda University, Advanced Research Institute for Science and Engineering, 17 Kikui-cho, Shinjuku-ku, Tokyo 162-0044, Japan*
[60]*Weizmann Institute, Rehovot 76100, Israel*
[61]*Institute for Particle and Nuclear Physics, Wigner Research Centre for Physics, Hungarian Academy of Sciences*
(Wigner RCP, RMKI) H-1525 Budapest 114, P.O. Box 49, Budapest, Hungary
[62]*Yonsei University, IPAP, Seoul 120-749, Korea*

The PHENIX experiment has measured electrons and positrons at midrapidity from the decays of hadrons containing charm and bottom quarks produced in $d +$ Au and $p + p$ collisions at $\sqrt{s_{NN}} =$ 200 GeV in the transverse-momentum range $0.85 \leq p_T^e \leq 8.5$ GeV/c. In central $d +$ Au collisions, the nuclear modification factor R_{dA} at $1.5 < p_T < 5$ GeV/c displays evidence of enhancement of these electrons, relative to those produced in $p + p$ collisions, and shows that the mass-dependent Cronin enhancement observed at the Relativistic Heavy Ion Collider extends to the heavy D meson family. A comparison with the neutral-pion data suggests that the difference in cold-nuclear-matter effects on light- and heavy-flavor mesons could contribute to the observed differences between the π^0 and heavy-flavor-electron nuclear modification factors R_{AA}.

The experimental collaborations at the Relativistic Heavy Ion Collider (RHIC) have established that a hot, dense medium with partonic degrees of freedom is formed in Au + Au collisions at $\sqrt{s_{NN}} = 200$ GeV [1–4]. The temperature achieved in this medium, as inferred from direct-photon measurements, is well over the threshold expected from lattice-quantum-chromodynamics calculations to enable deconfinement and create the quark gluon plasma [5]. Studies of the interactions of heavy quarks with this matter are of particular interest. Since charm and bottom quarks are dominantly produced by gluon fusion in the early stages of the collision, they experience the complete evolution of the system. The heavy-quark-production baseline in $p + p$ collisions at $\sqrt{s_{NN}} = 200$ GeV is consistent with fixed order plus next-to-leading-log perturbative quantum chromodynamics (QCD) calculations within uncertainties [6]. In central Au + Au collisions, suppression of electrons from the decays of hadrons containing heavy quarks has been measured relative to the yield in $p + p$ collisions scaled by the number of nucleon-nucleon collisions, N_{coll}, suggesting that heavy quarks lose a significant amount of their initial energy [7]. The positive elliptic flow amplitude of these decay electrons implies that heavy quarks flow along with the light partons that compose the bulk of the medium. When considered together, the suppression and elliptic flow of these quarks are in qualitative agreement with calculations based on Langevin transport models [8,9] that imply a viscosity to entropy density ratio close to the conjectured quantum lower bound of $1/4\pi$ [10].

A full understanding of these phenomena requires measurements of initial state effects inherent to nuclear collisions, which are present in Au + Au collisions but are difficult to distinguish experimentally from subsequent effects due to interactions with the hot medium. Compared to free protons and neutrons, the parton distribution functions inside the nucleus are significantly modified, and processes which originate from partonic

interactions can thereby also be modified [11]. Partons can also experience transverse momentum broadening via collisions inside the nucleus [12], or lose energy in the nuclear medium during the initial stages of a nuclear collision [13], before any thermalized system is formed. Together, these modifications inherent to collisions of nuclei may introduce so-called cold-nuclear-matter (CNM) effects on the observed particle spectra, which cannot be accounted for with a reference from $p + p$ data. It is therefore necessary to study $p +$ Au (or $d +$ Au) collisions, where a hot nuclear medium is not expected to form, to isolate these nuclear effects. Additional effects which are present in Au + Au collisions can then be attributed to the hot nuclear medium.

To this end, a vigorous experimental effort to quantify CNM effects is underway at RHIC. A mass-dependent Cronin enhancement has been observed for π, K, and p production [14,15], where the p_T spectra of these hadrons in $d +$ Au collisions are hardened with respect to $p + p$ collisions. While overall J/ψ production is suppressed in $d +$ Au collisions, a broadening of the p_T spectrum is also observed [16,17]. The relative strengths and centrality dependence of initial-state effects and breakup in the cold nuclear medium that contribute to these phenomena are not known. The study of mesons containing open heavy flavor can help disentangle these coexisting effects. This Letter presents measurements of p_T spectra and the nuclear modification factor (R_{dA}) of electrons and positrons from the decays of hadrons containing charm and bottom quarks ($e_{\text{HF}}^{\pm}$) produced in $d +$ Au collisions at $\sqrt{s_{NN}} = 200$ GeV. When combined with heavy-quark measurements from $p + p$ and Au + Au collisions, this analysis provides a detailed study of the production of heavy quarks, the effects of production in a nucleus, and the dynamics of the hot nuclear medium.

The PHENIX experiment [18] sampled 80 nb^{-1} of integrated luminosity during the 2008 $d +$ Au run at RHIC, a

factor of 30 increase over the 2003 $d + $Au data set. The minimum bias (MB) trigger and event centrality are obtained from two beam-beam counters located at $3.1 < |\eta| < 3.9$ in pseudorapidity. The charge generated in the beam-beam counter facing the incoming Au nucleus is divided into four categories covering the 0–20%, 20–40%, 40–60%, and 60–88% most central collisions. As the MB-trigger efficiency is $88 \pm 4\%$ of the total $d + $Au inelastic cross section, a correction factor is applied to the yield measured in the MB-triggered data sample to give a nonbiased sample, covering 100% of the $d + $Au collision centrality.

This analysis considers electrons and positrons identified in the two PHENIX central arm spectrometers. Each arm covers an azimuthal angle $\Delta\phi = \pi/2$ and a pseudorapidity range $|\eta| < 0.35$, and uses layers of multiwire proportional chambers and pad chambers for charged particle tracking. Ring-imaging Čerenkov (RICH) counters and electromagnetic calorimeters (EMCal) provide electron-identification and hadron-rejection capabilities. A coincidence of the MB trigger and a RICH hit matched with an energy deposit of at least 600 or 800 MeV in the EMCal functions as an electron trigger. At $p_T = 5$ GeV/c, charged pions begin to radiate in the RICH counters, but matching requirements between the track's energy deposit in the EMCal and reconstructed momentum effectively eliminate hadron contamination out to $p_T = 8$ GeV/c. Above this, hadronic contamination accounts for $20 \pm 10\%$ of the signal, and is subtracted. A full GEANT simulation of the PHENIX detector is used to correct for the incomplete azimuthal acceptance and electron-identification efficiency of the central-arm detectors.

Most of the electrons produced in collisions at RHIC come not from heavy-flavor decays, but from the neutral-pion Dalitz decay, $\pi^0 \to \gamma e^+ e^-$. The η Dalitz decay contributes about 10% of the electron background for $1 < p_T < 9$ GeV/c. Other hadron decays (η', ρ, ω, ϕ, Υ) add to the background at the few percent level. Internal and external conversions of direct photons, while negligible at $p_T < 2$ GeV/c, are significant sources of electrons at high momentum. Electrons from the decay $J/\psi \to e^+ e^-$ are a significant source of background at intermediate p_T, and constitute a maximum of about 25% of the total electron background at $p_T = 5$ GeV/c. Conversions of photons from hadron decays are significant at all momenta; however, the low material design of the PHENIX detector ensures that the number of these conversion electrons is less than half of that from neutral-pion Dalitz decay. In addition, electrons produced at displaced vertices from the K_{e3} decays of K mesons are misreconstructed by the PHENIX tracking algorithm and contribute about 3% of the total background at $p_T = 0.85$ GeV/c, but quickly fall off to less than 1% at $p_T = 1.5$ GeV/c.

Two independent methods are used to isolate the contribution of heavy flavor electrons. The cocktail method uses a Monte Carlo hadron decay generator to calculate the electron background from each relevant hadron species. The parametrization of the neutral-pion p_T spectrum is determined by a modified Hagedorn fit to pion data obtained from earlier measurements in $d + $Au collisions [14,19]. The shape of the p_T spectra of the other mesons is determined by m_T scaling the pion fit, that is, the variable substitution $p_T \to m_T = \sqrt{p_T^2 + (M_{\text{meson}}^2 - m_{\pi^0}^2)}$, and their normalization is set to world averages of the ratio of meson/π^0 at high momentum [19,20]. Direct-photon contributions are estimated by scaling the measured direct-photon yield in $p + p$ collisions by N_{coll} [21]. The number of conversion electrons is found by a full GEANT simulation of the PHENIX detector material, and a similar simulation, in conjunction with the actual PHENIX tracking algorithm, is used to estimate the K_{e3} decay background. Contributions from J/ψ decays are found by parametrizing the measured J/ψ spectrum from Ref. [16] for each centrality, for $d + $Au collisions, and from Ref. [22] for $p + p$ collisions. The small background due to Υ decays and the Drell-Yan process are taken from Ref. [23], and scaled by N_{coll} for each centrality. The sum of these background sources is then subtracted from the inclusive electron measurement to give the heavy flavor contribution.

The second method of signal extraction is based on the fact that the vast majority of the background electrons are "photonic" in nature; i.e., they originate from either a real photon (the conversion electrons) or a virtual photon (the electrons from Dalitz decays), while signal electrons are nonphotonic. The inclusive yield of electrons in the standard detector configuration can be parametrized as

$$N_e^{\text{standard}} = N^\gamma + N^{\text{non}\gamma}, \tag{1}$$

where N^γ ($N^{\text{non}\gamma}$) represents the photonic (nonphotonic) electron yield. The addition of extra material (the "converter," a sheet of brass 1.68% of a radiation length thick, wrapped around the beam pipe) into the PHENIX aperture increases the photonic component by a factor R_γ, but attenuates the signal by an amount $(1 - \epsilon)$, giving a total yield

$$N_e^{\text{converter}} = R_\gamma N^\gamma + (1 - \epsilon)N^{\text{non}\gamma}. \tag{2}$$

By modeling the converter material in simulation, the factors R_γ and ϵ are determined to be $2.32 \pm 2.7\%$ (with a slight p_T dependence), and $0.021 \pm 25\%$, respectively. The inclusive yields N_e^{standard} and $N_e^{\text{converter}}$ are measured by the PHENIX spectrometer, so a simultaneous solution of Eqs. (1) and (2) gives the quantity of interest $N^{\text{non}\gamma}$. The nonphotonic background sources, namely K_{e3} decays and the dielectron decays of the ρ, ω, ϕ, J/ψ, and Υ contribute about 10% of the total background at $p_T < 1$ GeV/c, and are subtracted following the cocktail method described above. The converter method provides a robust but statistics-limited determination of the photonic background. Since the converter material creates an undesirable background for other measurements, only 3% of

the d + Au data recorded by PHENIX in 2008 was taken with the converter installed.

A crucial cross check of this measurement's accuracy is the consistency of these two independent background determination methods. A comparison of the photonic components of the cocktail (Dalitz decay electrons, conversions, and direct photons) to the photonic-electron signal extracted by the converter method shows agreement within 8% for all centralities (see the inset of Fig. 1). Since the converter method gives a direct measurement of the photonic background, while the cocktail is a calculation that relies on simulation, the photonic components of the cocktail are scaled to match the converter data in each centrality by factors ranging from 0.92 to 1.01. Detailed descriptions of these methods can be found in Ref. [23].

Figure 1 shows the p_T spectrum of electrons from open heavy flavor decays for each d + Au centrality bin, and for p + p collisions that were measured during the same RHIC run period with identical techniques. The heavy flavor electron yield is determined by the cocktail method, with photonic components scaled to match the converter data. The statistical (systematic) uncertainties are shown as bars (boxes) around the central values. The boxes contain the uncertainties in the solid angle correction, electron-identification efficiency, and trigger-bias correction. Added in quadrature with those is the uncertainty from the cocktail subtraction. The lines are a fixed-order plus

next-to-leading-logarithm spectral shape [24] fitted to a previous p + p heavy-flavor electron measurement [23], scaled by N_{coll} for each centrality. The p + p data presented here are in good agreement with our previous p + p results; however, the statistical uncertainties on the new data are ~2 times larger. Fitting a constant to the ratio of the new data to the old yields a value of 0.97 ± 0.02, with χ^2 per degree of freedom equal to 20.3/26. The fact that the 2008 p + p data agree with the previous p + p data provides an important cross check on the methods used to extract the 2008 d + Au $e^{\pm}_{HF}$ spectra.

Due to changes in the detector configuration that resulted in increased photon conversion background at low p_T, the signal to background at low p_T is not as good as it was in previous measurements. Coupled with the fact that ~90% of the electrons from charmed hadron decays fall below $p_T = 0.8$ GeV/c, where the present data cut off, this means that the data do not place meaningful constraints on the total charm production cross section.

The d + Au electron spectra are directly compared to the p + p reference data by computing

$$R_{dA} = \frac{dN^e_{dA}/dp_T}{\langle N_{coll} \rangle \times dN^e_{pp}/dp_T} \qquad (3)$$

for each centrality. Figure 2 shows R_{dA} as a function of p_T for the most-peripheral and most-central centrality bins. As in Fig. 1, the statistical (systematic) uncertainties are represented by bars (boxes). For points at $p_T < 1.6$ GeV/c, R_{dA} is found by dividing point by point the d + Au yield by the p + p yield from Ref. [23]. At higher transverse momentum, where the p + p heavy-flavor electron spectrum is consistent with a shape from perturbative QCD, a fit to the spectral shape from the Ref. [24] calculations is used to
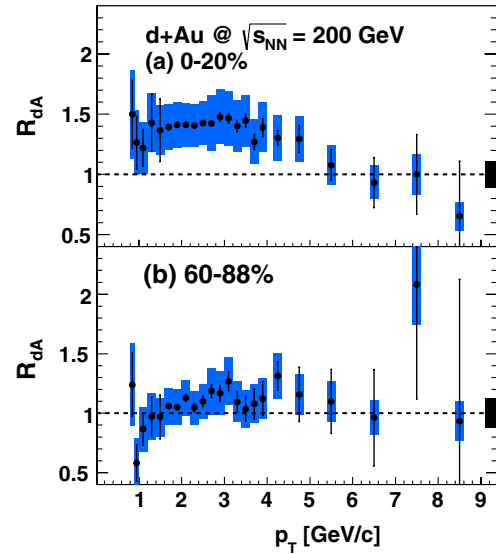

FIG. 1 (color online). Electrons from heavy flavor decays, separated by centrality. The lines represent a fit to the previous p + p result [23], scaled by N_{coll}. The inset shows the ratio of photonic background electrons determined by the converter and cocktail methods for minimum bias d + Au collisions, with error bars (boxes) that represent the statistical uncertainty on the converter data (systematic uncertainty on the photonic-electron cocktail). See text for details on uncertainties.

FIG. 2 (color online). The nuclear modification factor, R_{dA}, for electrons from open heavy flavor decays, for the (a) most central and (b) most peripheral centrality bins.

represent the $p + p$ yield. The statistical uncertainty on the fit is included as a systematic uncertainty on the shape of R_{dA} by adding it in quadrature with the systematic uncertainties on the electron background subtraction and solid angle and efficiency corrections. The global scaling uncertainty from the uncertainty in N_{coll} and the total sampled $p + p$ luminosity is given by a box on the right. Note that the 2008 $p + p$ data shown in Fig. 1 could be used for the denominator of R_{dA}; however, the use of the more precise data from Ref. [23] gives a smaller uncertainty on R_{dA}.

The central R_{dA} shows an enhancement out to $p_T \approx 5$ GeV/c, and implies that the suppression of heavy flavor electrons in central Au + Au collisions at RHIC is not an initial state CNM effect, but rather is due to the hot nuclear medium. The peripheral nuclear modification factor also shows some evidence of an enhancement, which is to be expected since even the most peripheral centrality bin in $d + $Au samples a significant nuclear thickness. Although the techniques used here do not allow separation of electrons from charm and bottom decays from each other, measurements from $p + p$ collisions show that $p_T = 5$ GeV/c is near the transition point where contributions from bottom quarks begin to dominate over charm [25]. Since the total charm cross section is expected to scale with N_{coll}, this enhancement below 5 GeV/c suggests a p_T broadening of the D spectral shape, with a mass dependence that roughly follows the previously observed trend in the π, K, and p families. The B spectrum may also be modified; however, the uncertainties on the data and on the relative D and B contributions to the electron spectra preclude a precise determination of any effects.

The effects of cold nuclear matter are expected to be present in the initial state of $A + A$ collisions; however, this CNM enhancement is convolved with the suppressing

effects of hot nuclear matter. Figure 3 shows R_{dA} and R_{AA} for $e^{\pm}_{HF}$ and the neutral pion, for which only small CNM effects are observed [19,26]. Above $p_T \approx 5$ GeV/c, where the CNM effects on both species are small, their R_{AA} values are consistent within uncertainties. However, in the range where CNM enhancement is large for $e^{\pm}_{HF}$ and small on π^0, the corresponding $e^{\pm}_{HF}R_{AA}$ values are consistently above the π^0 values. This could suggest that the difference in the initial state cold nuclear matter effects due to the mass-dependent Cronin enhancement is reflected in the final state spectra of these particles in Au + Au collisions, although alternate explanations involving mass-dependent partonic energy loss in the hot medium are not ruled out.

In summary, we have observed an enhancement of electrons from heavy-flavor decays produced in central $d + $Au collisions at $\sqrt{s_{NN}} = 200$ GeV. The previously observed suppression of these electrons in central Au + Au collisions is therefore attributed to hot-nuclear-matter effects. We find that the π^0 and $e^{\pm}_{HF}$ nuclear modification factors R_{AA} are consistent within uncertainties in the p_T range where CNM effects on both species are small. In the range where CNM enhancement of $e^{\pm}_{HF}$ is significant in $d + $Au collisions, these effects may also be apparent in the Au + Au data.
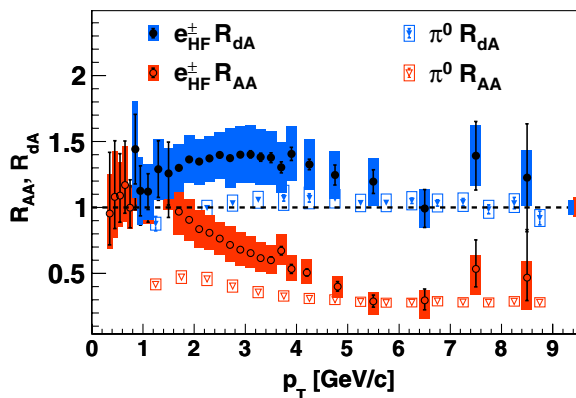
FIG. 3 (color online). The nuclear modification factors R_{dA} and R_{AA} for minimum bias $d + $Au and Au + Au collisions, for the π^0 and $e^{\pm}_{HF}$. The two boxes on the right side of the plot represent the global uncertainties in the $d + $Au (left) and Au + Au (right) values of N_{coll}. An additional common global scaling uncertainty of 9.7% on R_{dA} and R_{AA} from the $p + p$ reference data is omitted for clarity.

*Deceased.

†PHENIX Spokesperson.
jacak@skipper.physics.sunysb.edu

[1] K. Adcox *et al.* (PHENIX Collaboration), Nucl. Phys. **A757**, 184 (2005).

[2] I. Arsene *et al.* (BRAHMS Collaboration), Nucl. Phys. **A757**, 1 (2005).

[3] B. B. Back *et al.* (PHOBOS Collaboration), Nucl. Phys. **A757**, 28 (2005).

[4] J. Adams *et al.* (STAR Collaboration), Nucl. Phys. **A757**, 102 (2005).

[5] A. Adare *et al.* (PHENIX Collaboration), Phys. Rev. Lett. **104**, 132301 (2010).

[6] A. Adare *et al.* (PHENIX Collaboration), Phys. Rev. Lett. **97**, 252002 (2006).

[7] A. Adare *et al.* (PHENIX Collaboration), Phys. Rev. Lett. **98**, 172301 (2007).

[8] G. D. Moore and D. Teaney, Phys. Rev. C **71**, 064904 (2005).

[9] H. van Hees, V. Greco, and R. Rapp, Phys. Rev. C **73**, 034913 (2006).

[10] P. K. Kovtun, D. T. Son, and A. O. Starinets, Phys. Rev. Lett. **94**, 111601 (2005).

[11] K. J. Eskola, H. Paukkunen, and C. A. Salgado, J. High Energy Phys. 04 (**2009**) 065.

[12] R. Vogt, Int. J. Mod. Phys. E **12**, 211 (2003).

[13] I. Vitev, Phys. Rev. C **75**, 064906 (2007).

[14] S. S. Adler *et al.* (PHENIX Collaboration), Phys. Rev. C **74**, 024904 (2006).

[15] J. Adams *et al.* (STAR Collaboration), Phys. Lett. B **637**, 161 (2006).

[16] A. Adare *et al.* (PHENIX Collaboration), arXiv:1204.0777.

[17] A. Adare *et al.* (PHENIX Collaboration), Phys. Rev. Lett. **107**, 142301 (2011).

[18] K. Adcox *et al.* (PHENIX Collaboration), Nucl. Instrum. Methods Phys. Res., Sect. A **499**, 469 (2003).

[19] S. S. Adler *et al.* (PHENIX Collaboration), Phys. Rev. Lett. **98**, 172302 (2007).

[20] K. Nakamura *et al.* (Particle Data Group), J. Phys. G **37**, 075021 (2010).

[21] S. S. Adler *et al.* (PHENIX Collaboration), Phys. Rev. Lett. **98**, 012002 (2007).

[22] A. Adare *et al.* (PHENIX Collaboration), Phys. Rev. D **82**, 012001 (2010).

[23] A. Adare *et al.* (PHENIX Collaboration), Phys. Rev. C **84**, 044905 (2011).

[24] M. Cacciari, P. Nason, and R. Vogt, Phys. Rev. Lett. **95**, 122001 (2005).

[25] A. Adare *et al.* (PHENIX Collaboration), Phys. Rev. Lett. **103**, 082002 (2009).

[26] A. Adare *et al.* (PHENIX Collaboration), Phys. Rev. Lett. **101**, 232301 (2008).